The chloride intracellular channel protein CLIC4 inhibits filopodium formation induced by constitutively active mutants of formin mDia2

Elisabetta Argenzio[1] and Metello Innocenti[2] (iD)

1 Division of Cell Biology, The Netherlands Cancer Institute, Amsterdam, The Netherlands
2 Heidelberg University Biochemistry Center (BZH), Heidelberg University, Germany

Correspondence
M. Innocenti, Heidelberg University Biochemistry Center (BZH), Heidelberg University, Im Neuenheimer Feld 328, 69120 Heidelberg, Germany
Tel: +496221544287
E-mails: metello.innocenti@bzh.uni-heidelberg.de; metelloinnocenti@gmail.com

Chloride intracellular channel 4 (CLIC4) functions in diverse actin-dependent processes. Upon Rho activation, CLIC4 reversibly translocates from the cytosol to the plasma membrane to regulate cell adhesion and migration. At the plasma membrane, CLIC4 counters the formation of filopodia, which requires actin assembly by the formin mammalian Diaphanous (mDia)2. To this end, mDia2 must be activated through conversion from the closed to the open conformation. Thus, CLIC4 could harness the activation or the open conformation of mDia2 to inhibit filopodium formation. Here, we find that CLIC4 silencing enhances the filopodia induced by two constitutively active mDia2 mutants. Furthermore, we report that CLIC4 binds the actin-regulatory region of mDia2 *in vitro*. These results suggest that CLIC4 modulates the activity of the open conformation of mDia2, shedding new light into how cells may control filopodia.

Keywords: actin; CLIC4; cytoskeleton; filopodia; formins; mDia2

Chloride intracellular channel (CLIC) proteins (CLIC1–6) are globular proteins of about 28 kDa, structurally resembling omega-class glutathione S-transferases (GSTOs) [1-4]. Yet, CLIC proteins neither function as conventional chloride channels nor do they behave like GSTOs. Instead, they play a role in several actin-dependent processes, such as tubulogenesis, membrane remodeling, endosomal trafficking, vacuole formation, and cell adhesion [3-5]. Moreover, some of the CLICs (CLIC3-5) are associated with the cortical actin cytoskeleton and control intracellular vesicular compartments by modulating actin-mediated vesicle trafficking [5-9]. In particular, CLIC4 has a homogeneous distribution in the cytosol with enrichment on a subset of early and recycling endosomes, and some plasma membrane patches [8,10,11]. In response to agonists activating the small Rho-GTPase Rho [8,10,12,13], CLIC4 rapidly and reversibly translocates from the cytosol to the plasma membrane. CLIC4 translocation requires the interaction with G-actin-binding protein profilin 1 and actin polymerization induced by Rho and mammalian Diaphanous (mDia) 2 (mDia2) formin [10]. At the plasma membrane, CLIC4 modulates β1 integrin trafficking, cell adhesion, and migration [8], and inhibits the protrusion of mDia2-induced filopodia [8,10].

mDia2 is widely expressed and one of the best-characterized formin family proteins, which are defined by a formin homology 1 (FH1) domain juxtaposed to a FH2 domain. Together, they make up a functional unit (FH1-FH2) that regulates actin polymerization [14–18]. Interaction of profilin 1 with the FH1 domain enables most formins to promote nucleation and elongation of linear actin filaments [14,18]. In mDia2, a Diaphanous

inhibitory domain (DID) and a Diaphanous autoregulatory domain (DAD) flank the FH1-FH2 at the N- and the C-terminal side, respectively, bind to each other, and therefore keep mDia2 in a closed conformation, which prevents actin polymerization [14,18]. Active, GTP-bound RhoA-C and RhoF associate with Rho-GTPase-binding domain (GBD), which is partially overlapping with the DID [14,18]. This weakens the DID-DAD interaction, thus relieving mDia2 autoinhibition. Also, small GTPase Cdc42 can activate mDia2, as GTP-bound Cdc42 binds to a partial Cdc42- and Rac-interactive binding motif encased in the GBD of mDia2 [19]. Of note, Cdc42 is a pivotal regulator of filopodia, finger-like protrusions made up of a bundle of linear actin filaments [20], and mDia2 functions as a key effector of both Cdc42 and RhoF in filopodium formation [21-23].

Contrary to the well-characterized mDia2 activation mechanism involving the conversion from the closed to the open conformation, the regulation of active mDia2 remains poorly understood. In this regard, it is known that profilin 1 increases the processivity and the actin-filament elongation rate of mDia2 *in vitro* [24]. Furthermore, recent data show that CLIC4 restrains mDia2-driven filopodium formation by restricting filopodial tip protrusion [10]. This raises the possibility that CLIC4 could counter the activation or the open conformation of mDia2. Here, we have tested this hypothesis by leveraging point mutations and deletions that relieve mDia2 autoinhibition. We show that CLIC4 restricts the formation of filopodia induced by two constitutively active mDia2 mutants and also binds to the actin-regulatory FH1-FH2 region of mDia2 *in vitro*. These results jointly suggest that CLIC4 acts on the open conformation of mDia2 to inhibit filopodium formation.

Materials and methods

Reagents and antibodies

Type I collagen was from Inamed BioMaterials (Fremont, CA, USA). EDTA-free protease inhibitor cocktail tablets were from Roche Pharma (Basel, Switzerland). Phalloidin red (actin-stain™ 555 Phalloidin) was from Cytoskeleton, Inc (Denver, CO, USA). Antibodies used were as follows: mouse anti-FLAG M2 (Sigma-Aldrich, Taufkirchen, Germany), mouse anti-GST (Santa Cruz Biotechnology, Dallas, TX, USA), and anti-mouse Alexa Fluor™ 488-conjugated secondary antibodies (Invitrogen).

Vectors

pCDNA3 FLAG-mDia2 (FH1-FH2), pCDNA3 FLAG-mDia2 MA, and pGEX-6P1-mDia2 (FH1-FH2) were

previously described [22,25]. pGEX-6P1-CLIC4 wt and the C35A mutant were previously described [8].

Cell Culture, knockdowns, and transfections

HeLa cells were grown in Dulbecco's modified Eagle's medium (DMEM; Thermo Fisher Scientific, Waltham, MA, USA) supplemented with 10% FBS under 5% CO_2 at 37 °C. Stable CLIC4 knockdown HeLa cells were previously described and characterized [8,10]: In brief, shRNA TRCN0000044360 (#3) and TRCN0000044362 (#5) (TRC human shRNA library; Sigma) targeting human CLIC4, or the corresponding empty lentiviral vector (control knockdown) was used, along packaging vectors, to generate lentiviral particles upon transient transfection in HEK293T cells. Viruses were collected 48 h after transfection. CLIC4 stable knockdown and control cells were selected and maintained in medium with 2 $\mu g \cdot mL^{-1}$ puromycin. Plasmid transfections were performed with X-tremeGene 9 (Roche) reagent according to the manufacturer's instructions.

Recombinant proteins

GST-tagged CLIC4 was expressed in BL21 *Escherichia coli* and purified using Glutathione Sepharose® 4B beads (GE Healthcare Europe, Freiburg, Germany) and gel filtration as previously described [10]. GST was removed with PreScission Protease (GE Healthcare). GST-tagged FH1-FH2 region of mDia2 was expressed in BL21 *E. coli* and purified using Glutathione Sepharose® 4B beads (GE Healthcare) as previously described [22,26,27], whereas GST was removed with PreScission Protease (GE Healthcare) as described for profilin 1 [16].

Pull-down assays

Purified recombinant proteins containing the GST moiety were immobilized on Glutathione Sepharose® 4B beads (GE Healthcare) and used as baits. Purified recombinant proteins without GST tag were used as preys. The pull-down assays were performed in NET buffer [16] supplemented with 1 mM DTT and EDTA-free protease inhibitor cocktail as previously described [22,26,27].

Western blotting

The pulled-down material was solubilized in Laemmli sample buffer (2% SDS, glycerol 10%, 62.5 mM Tris/HCl, pH 6.8, 5% 2-mercaptoethanol, and 0.002% bromophenol blue), boiled at 100 °C for 5 min, separated by SDS/PAGE, and then transferred on a nitrocellulose membrane (0.2 μm pore size; Whatman, GE Healthcare Europe). After transfer, membranes were blocked in nonfat dry milk and incubated with primary antibodies according to the manufacturer's

instructions, followed by HRP-conjugated secondary antibodies (1 : 10 000; Dako, Inc., Jena, Germany).

Imaging and analysis of filopodia

Control KD and CLIC4 KD cells were plated on collagen-coated coverslips and, one day later, starved overnight in DMEM supplemented with 0.1% FBS. Cells were fixed in 4% PFA dissolved in PEM buffer [28,29], permeabilized, and stained as previously described [17]. A CLSM Leica TCS SP5 operated with Leica Confocal Software (LAS-AF; Leica Microsystems, Wetzlar, Germany) and set on the sequential mode was used to acquire all images.

Filopodium length was measured manually using IMAGEJ (https://imagej.nih.gov) as explained previously [10]. For quantification of length, we considered genuine filopodia-only finger-like structures of at least 1.5 μm [22]. Filopodium density (ratio between the number of filopodia and the total cell perimeter in a given image) was determined using FiloQuant ImageJ plugin as explained previously [10]. For quantification of density, no cutoff was set.

Densitometry

To estimate band intensities, nonsaturated exposures of western blots were subjected to densitometric analyses using IMAGEJ (https://imagej.nih.gov). Normalized CLIC4 expression was determined as follows: The intensities of CLIC4 and of a housekeeping protein (e.g., actin) were determined by densitometry, and the CLIC4/housekeeping protein ratio was calculated for each lane. These values were then normalized taking that of the control knockdown lane as a reference. Normalized CLIC4 binding was determined as follows: The intensities of CLIC4 were determined by densitometry, and the obtained values were then normalized taking that of the input lane as a reference.

Statistical analyses

For determination of statistical significance, unpaired two-tailed Student's t-test and one-way ANOVA were performed using GRAPHPAD PRISM 7 software San Diego, CA, USA. Significance values are compared either with control conditions or with each other.

Results

CLIC4 restricts filopodium formation induced by constitutively active mDia2 mutants

Mutation of methionine 1041 within the DAD (M1041-to-A mutation, hereafter referred to as MA) is known to prevent the DID-DAD interaction and mDia2 autoinhibition [30] (Fig. 1). Consistently, expression of mDia2 MA has been shown to induce the formation of filopodia in a variety of cell lines [15-16,30,31] (Fig. 1). The same phenotype is elicited also by the isolated FH1-FH2 of mDia2, which is constitutively active in vitro and cannot bind to Rho-GTPases [10,18,22] (Fig. 1).

mDia2 MA and the FH1-FH2 of mDia2 were transfected in control and CLIC4 knockdown HeLa cells ([8,10] and Fig. S1), the latter forming longer and more abundant filopodia [10]. To carry out reliable single-cell morphometric analyses, we compared only cells that expressed these constructs at similar low anti-Flag intensity levels.

We observed that mDia2 MA stimulated the formation of filopodia in control knockdown HeLa cells and was enriched at their tip (Fig. 2A), as previously reported [10]. Filopodial density was higher in mDia2 MA-expressing cells compared with mock-transfected control cells, whereas filopodia were only slightly longer (Fig. S2A-B). mDia2 MA-dependent filopodia could be observed also upon silencing of CLIC4 (Fig. 2A), with their length and density being significantly increased compared with those measured in control knockdown cells (Fig. 2B). These observations suggest that CLIC4 regulates the open conformation of mDia2 and confirm that CLIC4 restrains the formation of mDia2-driven filopodia [10].

We sought to strengthen this notion and used the FH1-FH2 of mDia2, which is both constitutively active and irresponsive to Rho-GTPases (Fig. 1). This eliminates the potential effects that the increased basal activity of Rho and Cdc42 in CLIC4 knockdown cells may exert on both mDia2 MA and filopodium formation [10]. Expression of FH1-FH2 in control knockdown
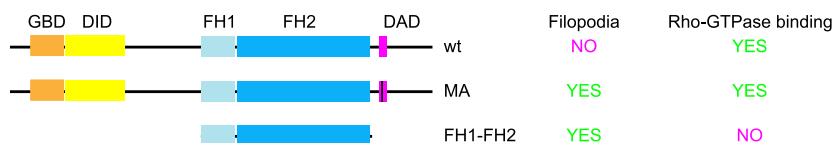
Fig. 1. Key features of the mDia2 mutants used in this study. Schematic representation of mDia2 and of the constructs used in this study. Colored boxes highlight key domains in wild-type mDia2 (wt; aa: 1–1172), the MA and FH1-FH2 mutants (FH1-FH2; aa: 530–1033). A black line marks the position of the M1041-to-A mutation in the DAD.

A

B
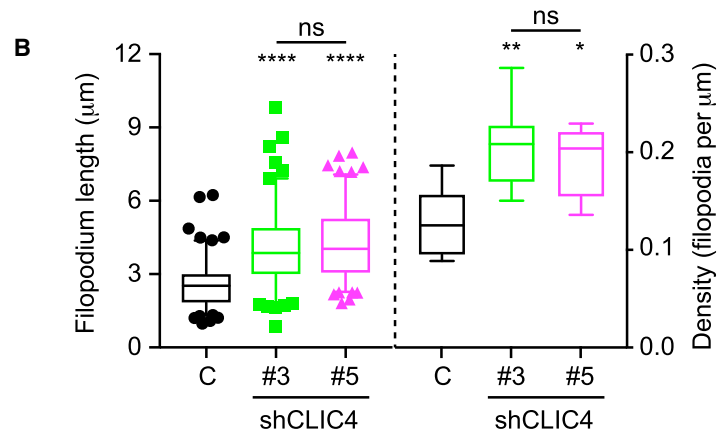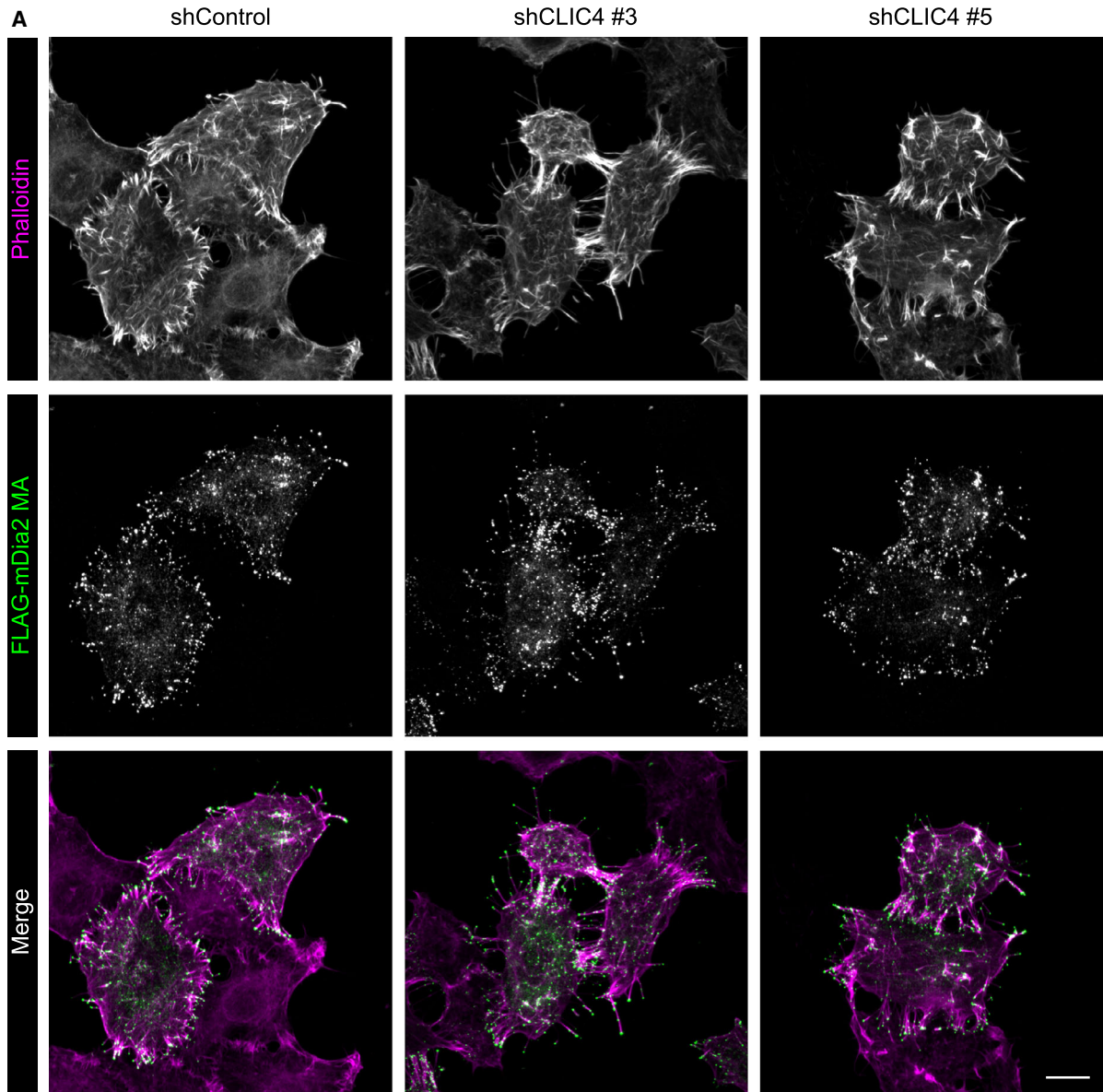
Fig. 2. CLIC4 regulates length and density of filopodia induced by mDia2 MA. (A) Control (shControl) and CLIC4 knockdown (shCLIC4 #3 and shCLIC4 #5) HeLa cells were seeded on collagen-I-coated coverslips, transfected with FLAG-tagged mDia2 MA, and serum-starved overnight. Representative compressed confocal Z-stacks of cells stained with phalloidin and anti-FLAG antibodies to detect F-actin (magenta in merge) and FLAG-mDia2 MA (green in merge), respectively. Scale bar, 10 μm. (B) Quantification of length and density of filopodia induced by mDia2 MA. Data represent filopodium length and density measured in three independent experiments as described in Materials and methods. Filopodial length (left): Box shows the 25th to 75th percentiles with line and whiskers indicating the median and the 5th and the 95th percentiles, respectively. Outliers are depicted as individual dots [$n_{shControl}$ = 16 cells (120 filopodia), $n_{shCLIC4\ \#3}$ = 22 cells (138 filopodia), $n_{shCLIC4\ \#5}$ = 19 (134 filopodia)]. Filopodial density (right): Box shows the 25th to 75th percentiles with line and whiskers indicating the median and the 5th and the 95th percentiles, respectively [$n_{shControl}$ = 20 cells (eight images), $n_{shCLIC4\ \#3}$ = 27 cells (nine images), $n_{shCLIC4\ \#5}$ = 26 (nine images)]. Ex post sample size calculations performed using the measured mean densities and SDs, and setting $P < 0.05$, gives a power > 95%. One-way ANOVA with Tukey's multiple comparisons test (*$P < 0.05$, **$P < 0.01$, and ****$P < 0.0001$, ns, nonsignificant).

cells increased both filopodial density and length with respect to mock-transfected cells (Fig. S2A,C). These results are in line with the ability of the FH1-FH2 to stimulate actin nucleation and elongation *in vitro*, and filopodium formation in cells [10,18,22]. The FH1-FH2 showed enrichment at the tip of filopodia like mDia2 MA, although most of the protein was in the nucleus (Fig. 3A), as previously reported [22]. More importantly, the filopodia triggered by the FH1-FH2 of mDia2 were longer in CLIC4 knockdown than in control cells (Fig. 3A,B). At variance with mDia2 MA, CLIC4 did not affect the density of FH1-FH2-induced filopodia in the CLIC4 knockdown cells (Fig. 3B). This and the observation that the filopodia induced by the FH1-FH2 are denser than those induced by mDia2 MA suggest that CLIC4 regulates mDia2 at multiple levels. In any case, these data show that CLIC4 can harness the activity of mDia2 after conversion to the open conformation. Moreover, they rule out that the previously reported filopodial phenotypes of the CLIC4 knockdown cells were merely due to the increased basal activity of Rho and Cdc42 [10].

CLIC4 binds to the FH1-FH2 of mDia2 *in vitro*

In line with this view, we found that purified recombinant CLIC4 and the FH1-FH2 region of mDia2 formed a complex *in vitro* (Fig. 4A). Parallel experiments conducted with CLIC4 C35A showed that this interaction does not require cysteine 35 (Fig. 4B), which is instead critical for profilin 1 binding and CLIC4 translocation to the plasma membrane [10]. However, we could not observe co-immunoprecipitation between endogenous mDia2 and CLIC4 in HeLa cells (data not shown) and previous studies failed to detect an association between CLIC4 and mDia2 in cell lysates [15,16]. Nevertheless, this interaction can potentially contribute to the activity of CLIC4 in filopodia as further explained below.

Discussion

Here, we have found that CLIC4 acts on the open conformation of mDia2 to inhibit filopodium formation. To this end, we have exploited two mDia2 mutants that are not autoinhibited, mDia2 MA and the isolated FH1-FH2 region. We showed that both mutants induce longer filopodia in cells silenced for CLIC4. While mDia2 MA-dependent filopodia are denser in the CLIC4 knockdown cells compared with the control ones, this is not the case for those induced by the FH1-FH2. This and the observation that the density of the FH1-FH2-induced filopodia is higher than that of the mDia2 MA-induced filopodia raise the enticing possibility that the disruption of the DID-DAD interaction is insufficient for full activation of mDia2. Detailed structure–function analyses of full-length mDia2 are awaited to clarify this issue. Whatever the case, it appears that the open conformation of mDia2 has at least two layers of CLIC4-dependent regulation.

Interestingly, we also found that CLIC4 binds physically to the FH1-FH2 of mDia2 and this interaction does not require cysteine 35. The lack of co-immunoprecipitation between endogenous CLIC4 and mDia2 along with proteomics studies listing profilins, but not CLIC4, in the mDia2 interactome [15,16] suggests that the CLIC4-mDia2 association occurs only at concentrations that can be achieved on intact membranes and/or is regulated by post-translational modifications in mammalian cells. Given that weak interactions control the activities of CLIC4 and mDia2 [3,10,18], we speculate that the CLIC4-mDia2 association will be functionally important at membrane sites of high local concentration of both proteins, such as the tip of filopodia. It is also intriguing that ubiquitination of the FH1 and FH2 domains of mDia2 has been reported *in vivo* [15,32] and future work should explore the role of mDia2 ubiquitination in CLIC4 binding and filopodium formation.
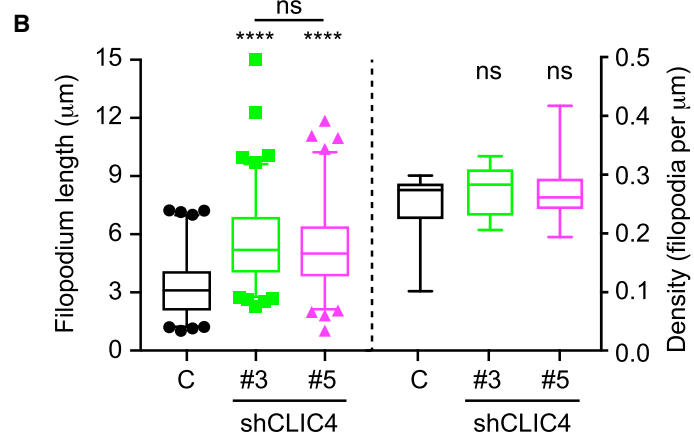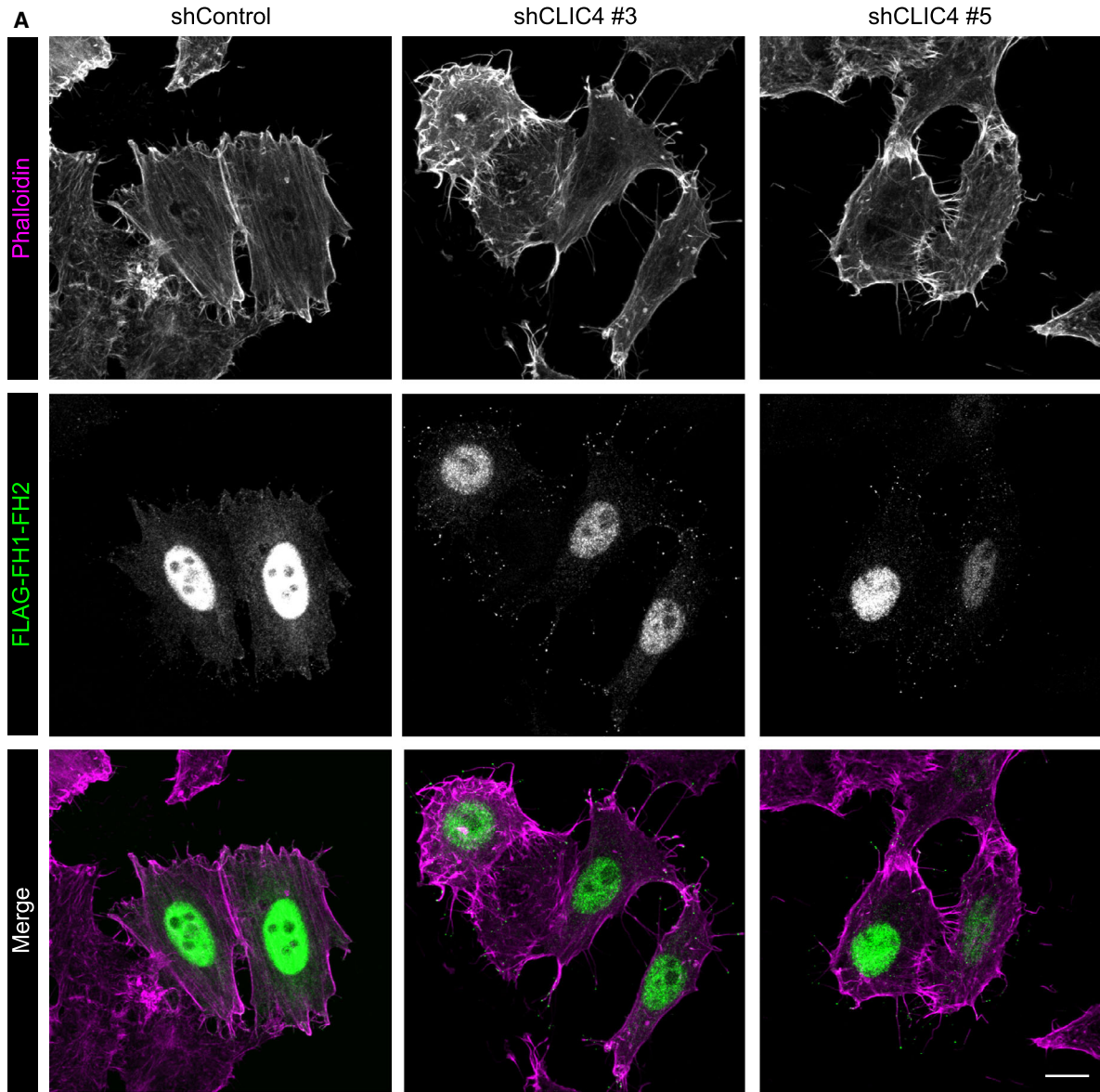
Fig. 3. CLIC4 regulates length and density of filopodia induced by the FH1-FH2 of mDia2. (A) Control (shControl) and CLIC4 knockdown (shCLIC4 #3 and shCLIC4 #5) HeLa cells were seeded on collagen-I-coated coverslips, transfected with FLAG-tagged FH1-FH2 of mDia2, and serum-starved overnight. Representative compressed confocal Z-stacks of cells stained with phalloidin and anti-FLAG antibodies to detect F-actin (magenta in merge) and FLAG-FH1-FH2 (green in merge), respectively. Scale bar, 10 µm. (B) Quantification of length and density of filopodia induced by the FLAG-FH1-FH2 of mDia2. Data represent filopodium length and density measured in three independent experiments as described in [Materials and methods]. Filopodial length (left): Box shows the 25th to 75th percentiles with line and whiskers indicating the median and the 5th and the 95th percentiles, respectively. Outliers are depicted as individual dots [$n_{shControl}$ = 12 cells (83 filopodia), $n_{shCLIC4 \#3}$ = 16 cells (101 filopodia), $n_{shCLIC4 \#5}$ = 14 cells (83 filopodia)]. Filopodial density (right): Box shows the 25th to 75th percentiles with line and whiskers indicating the median and the 5th and the 95th percentiles, respectively [$n_{shControl}$ = 13 cells (seven images), $n_{shCLIC4 \#3}$ = 19 cells (seven images), $n_{shCLIC4 \#5}$ = 19 (eight images)]. Ex post sample size calculations performed using the measured mean densities and SDs, and setting $P < 0.05$, indicate that about 100 images would be needed to obtain a power equal to 80%. One-way ANOVA with Tukey's multiple comparisons test (****$P < 0.0001$, ns, nonsignificant).
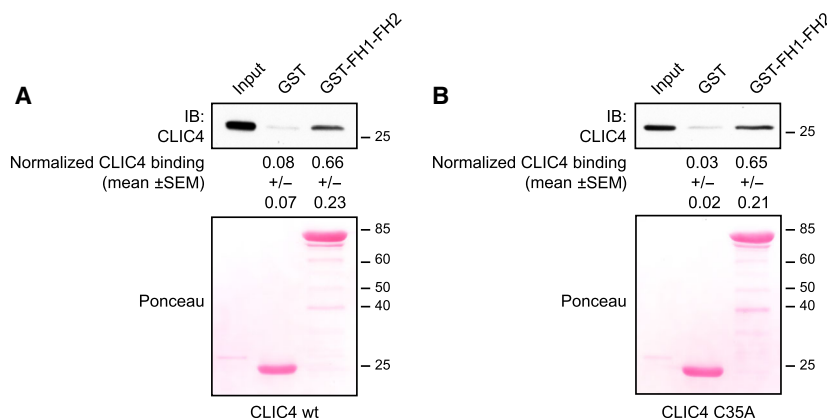
Fig. 4. CLIC4 binds the FH1-FH2 of mDia2 *in vitro*. (A) Purified immobilized GST-FH1-FH2 of mDia2 and GST (20 µM), as a control, were incubated with CLIC4 wt (50 µM) for 2 h on ice and pulled down with GST–agarose beads. Bound CLIC4 was detected by immunoblotting using anti-CLIC4 antibodies. Ponceau staining showed equal loading of the GST-fusion proteins. Data show representative results from one of three independent experiments. Normalized CLIC4 binding is reported (mean and SEM, unpaired *t*-test $P < 0.05$, $n = 3$). (B) Purified immobilized GST-FH1-FH2 of mDia2 and GST (20 µM), as a control, were incubated with CLIC4 C35A (50 µM) for 2 h on ice and pulled down with GST–agarose beads. Bound CLIC4 and loading were detected as in A. Data show representative results from one of three independent experiments. Normalized CLIC4 binding is reported (mean and SEM, unpaired *t*-test $P < 0.05$, $n = 3$).

In summary, these results suggest that CLIC4 modulates the function of the open conformation of mDia2 and pave the way for future studies that may shed new light into how cells control filopodia.

Acknowledgements

Author contributions

EA designed and performed experiments, and analysed data. MI designed experiments, analysed data and wrote the manuscript.

References

1 Harrop SJ, DeMaere MZ, Fairlie WD, Reztsova T, Valenzuela SM, Mazzanti M, Tonini R, Qiu MR, Jankova L, Warton K *et al*. (2001) Crystal structure of a soluble form of the intracellular chloride ion channel CLIC1 (NCC27) at 1.4-A resolution. *J Biol Chem* **276**, 44993–45000.

2 Dulhunty A, Gage P, Curtis S, Chelvanayagam G and Board P (2001) The glutathione transferase structural family includes a nuclear chloride channel and a ryanodine receptor calcium release channel modulator. *J Biol Chem* **276**, 3319–3323.

3 Argenzio E and Moolenaar WH (2016) Emerging biological roles of Cl- intracellular channel proteins. *J Cell Sci* **129**, 4165–4174.

4 Littler DR, Harrop SJ, Goodchild SC, Phang JM, Mynott AV, Jiang L, Valenzuela SM, Mazzanti M, Brown LJ, Breit SN *et al*. (2010) The enigma of the CLIC proteins: ion channels, redox proteins, enzymes, scaffolding proteins? *FEBS Lett* **584**, 2093–2101.

5 Jiang L, Phang JM, Yu J, Harrop SJ, Sokolova AV, Duff AP, Wilk KE, Alkhamici H, Breit SN, Valenzuela SM *et al*. (2014) CLIC proteins, ezrin, radixin, moesin and the coupling of membranes to the actin

cytoskeleton: a smoking gun? *Biochim Biophys Acta* **1838**, 643–657.

6 Berryman M, Bruno J, Price J and Edwards JC (2004) CLIC-5A functions as a chloride channel in vitro and associates with the cortical actin cytoskeleton *in vitro* and *in vivo*. *J Biol Chem* **279**, 34794–39801.

7 Berryman M and Bretscher A (2000) Identification of a novel member of the chloride intracellular channel gene family (CLIC5) that associates with the actin cytoskeleton of placental microvilli. *Mol Biol Cell* **11**, 1509–1521.

8 Argenzio E, Margadant C, Leyton-Puig D, Janssen H, Jalink K, Sonnenberg A and Moolenaar WH (2014) CLIC4 regulates cell adhesion and beta1 integrin trafficking. *J Cell Sci* **127**, 5189–5203.

9 Dozynkiewicz MA, Jamieson NB, Macpherson I, Grindlay J, van den Berghe PV, von Thun A, Morton JP, Gourley C, Timpson P, Nixon C *et al.* (2012) Rab25 and CLIC3 collaborate to promote integrin recycling from late endosomes/lysosomes and drive cancer progression. *Dev Cell* **22**, 131–145.

10 Argenzio E, Klarenbeek J, Kedziora KM, Nahidiazar L, Isogai T, Perrakis A, Jalink K, Moolenaar WH and Innocenti M (2018) Profilin binding couples chloride intracellular channel protein CLIC4 to RhoA-mDia2 signaling and filopodium formation. *J Biol Chem* **293**, 19161–19176.

11 Chou SY, Hsu KS, Otsu W, Hsu YC, Luo YC, Yeh C, Shehab SS, Chen J, Shieh V, He GA *et al.* (2016) CLIC4 regulates apical exocytosis and renal tube luminogenesis through retromer- and actin-mediated endocytic trafficking. *Nat Commun* **7**, 10412.

12 Ponsioen B, van Zeijl L, Langeslag M, Berryman M, Littler D, Jalink K and Moolenaar WH (2009) Spatiotemporal regulation of chloride intracellular channel protein CLIC4 by RhoA. *Mol Biol Cell* **20**, 4664–4672.

13 Shukla A, Malik M, Cataisson C, Ho Y, Friesen T, Suh KS and Yuspa SH (2009) TGF-beta signalling is regulated by Schnurri-2-dependent nuclear translocation of CLIC4 and consequent stabilization of phospho-Smad2 and 3. *Nat Cell Biol* **11**, 777–784.

14 Isogai T and Innocenti M (2016) New nuclear and perinuclear functions of formins. *Biochem Soc Trans* **44**, 1701–1708.

15 Isogai T, van der Kammen R, Bleijerveld OB, Goerdayal SS, Argenzio E, Altelaar AF and Innocenti M (2016) Quantitative proteomics illuminates a functional interaction between mDia2 and the proteasome. *J Proteome Res* **15**, 4624–4637.

16 Isogai T, van der Kammen R, Goerdayal SS, Heck AJ, Altelaar AF and Innocenti M (2015) Proteomic analyses uncover a new function and mode of action for mouse homolog of Diaphanous 2 (mDia2). *Mol Cell Proteomics* **14**, 1064–1078.

17 Isogai T, van der Kammen R and Innocenti M (2015) SMIFH2 has effects on formins and p53 that perturb the cell cytoskeleton. *Sci Rep* **5**, 9802.

18 Chesarone MA, DuPage AG and Goode BL (2010) Unleashing formins to remodel the actin and microtubule cytoskeletons. *Nat Rev Mol Cell Biol* **11**, 62–74.

19 Peng J, Wallar BJ, Flanders A, Swiatek PJ and Alberts AS (2003) Disruption of the Diaphanous-related formin Drf1 gene encoding mDia1 reveals a role for Drf3 as an effector for Cdc42. *Curr Biol* **13**, 534–545.

20 Jacquemet G, Hamidi H and Ivaska J (2015) Filopodia in cell adhesion, 3D migration and cancer cell invasion. *Curr Opin Cell Biol* **36**, 23–31.

21 Pellegrin S and Mellor H (2005) The Rho family GTPase Rif induces filopodia through mDia2. *Curr Biol* **15**, 129–133.

22 Beli P, Mascheroni D, Xu D and Innocenti M (2008) WAVE and Arp2/3 jointly inhibit filopodium formation by entering into a complex with mDia2. *Nat Cell Biol* **10**, 849–857.

23 Innocenti M (2018) New insights into the formation and the function of lamellipodia and ruffles in mesenchymal cell migration. *Cell Adh Migr* 1–41.

24 Cao L, Kerleau M, Suzuki EL, Wioland H, Jouet S, Guichard B, Lenz M, Romet-Lemonne G and Jegou A (2018) Modulation of formin processivity by profilin and mechanical tension. *eLife* **7**. e34176. https://doi.org/10.7554/eLife.34176

25 Isogai T, van der Kammen R, Leyton-Puig D, Kedziora KM, Jalink K and Innocenti M (2015) Initiation of lamellipodia and ruffles involves cooperation between mDia1 and the Arp2/3 complex. *J Cell Sci* **128**, 3796–3810.

26 van der Kammen R, Song JY, de Rink I, Janssen H, Madonna S, Scarponi C, Albanesi C, Brugman W and Innocenti M (2017) Knockout of the Arp2/3 complex in epidermis causes a psoriasis-like disease hallmarked by hyperactivation of transcription factor Nrf2. *Development* **144**, 4588–4603.

27 Galovic M, Xu D, Areces LB, van der Kammen R and Innocenti M (2011) Interplay between N-WASP and CK2 optimizes clathrin-mediated endocytosis of EGFR. *J Cell Sci* **124**, 2001–2012.

28 Leyton-Puig D, Kedziora KM, Isogai T, van den Broek B, Jalink K and Innocenti M (2016) PFA fixation enables artifact-free super-resolution imaging of the actin cytoskeleton and associated proteins. *Biol Open* **5**, 1001–1009.

29 Leyton-Puig D, Isogai T, Argenzio E, van den Broek B, Klarenbeek J, Janssen H, Jalink K and Innocenti M (2017) Flat clathrin lattices are dynamic actin-controlled hubs for clathrin-mediated endocytosis and signalling of specific receptors. *Nat Commun* **8**, 16068.

30 Wallar BJ, Stropich BN, Schoenherr JA, Holman HA, Kitchen SM and Alberts AS (2006) The basic region of

the diaphanous-autoregulatory domain (DAD) is required for autoregulatory interactions with the diaphanous-related formin inhibitory domain. *J Biol Chem* **281**, 4300–4307.

31 Barzik M, McClain LM, Gupton SL and Gertler FB (2014) Ena/VASP regulates mDia2-initiated filopodial length, dynamics, and function. *Mol Biol Cell* **25**, 2604–2619.

32 DeWard AD and Alberts AS (2009) Ubiquitin-mediated degradation of the formin mDia2 upon completion of cell division. *J Biol Chem* **284**, 20061–20069.

Supporting information

Additional supporting information may be found online in the Supporting Information section at the end of the article.

Fig. S1. Validation of CLIC4 knockdown.

Fig. S2. Characterization of the filopodia induced by mDia2 MA and by the FH1-FH2 region.